Functional and Biochemical Analysis of the Type 1 Inositol (1,4,5)-Trisphosphate Receptor Calcium Sensor

Huiping Tu,* Elena Nosyreva,* Tomoya Miyakawa,† Zhengnan Wang,* Akiko Mizushima,† Masamitsu Iino,† and Ilya Bezprozvanny*

*Department of Physiology, University of Texas Southwestern Medical Center at Dallas, Dallas, Texas USA; and †Department of Pharmacology, Graduate School of Medicine, The University of Tokyo, Tokyo, Japan

ABSTRACT Modulation of the type 1 inositol (1,4,5)-trisphosphate receptors ($InsP_3R1$) by cytosolic calcium (Ca^{2+}) plays an essential role in their signaling function, but structural determinants and mechanisms responsible for the $InsP_3R1$ regulation by Ca^{2+} are poorly understood. Using DT40 cell expression system and Ca^{2+} imaging assay, in our previous study we identified a critical role of E2100 residue in the $InsP_3R1$ modulation by Ca^{2+}. By using intrinsic tryptophan fluorescence measurements in the present study we determined that the putative $InsP_3R1$ Ca^{2+}-sensor region (E1932–R2270) binds Ca^{2+} with 0.16 μM affinity. We further established that E2100D and E2100Q mutations decrease Ca^{2+}-binding affinity of the putative $InsP_3R1$ Ca^{2+}-sensor region to 1 μM. In planar lipid bilayer experiments with recombinant $InsP_3R1$ expressed in *Spodoptera frugiperda* cells we discovered that E2100D and E2100Q mutations shifted the peak of the $InsP_3R1$ bell-shaped Ca^{2+} dependence from 0.2 μM to 1.5 μM Ca^{2+}. In agreement with the biochemical data, we found that the apparent affinities of Ca^{2+} activating and inhibitory sites of the $InsP_3R1$ were 0.2 μM for the wild-type channels and 1–2 μM Ca^{2+} for the E2100D and E2100Q mutants. The results obtained in our study support the hypothesis that E2100 residue forms a part of the $InsP_3R1$ Ca^{2+} sensor.

INTRODUCTION

The inositol (1,4,5)-trisphosphate receptor ($InsP_3R$) is an intracellular calcium (Ca^{2+}) release channel that plays a critical role in Ca^{2+} signaling (Berridge, 1993). Three mammalian isoforms of $InsP_3R$—type I ($InsP_3R1$), type II ($InsP_3R2$), and type III ($InsP_3R3$)—have been identified (Furuichi et al., 1994), with only limited information available to date about differences in their functional properties (Miyakawa et al., 1999; Thrower et al., 2001). The $InsP_3R$ are subjected to multiple levels of regulation (Berridge, 1993; Bezprozvanny and Ehrlich, 1995; Taylor, 1998). Binding of $InsP_3$ triggers the $InsP_3R$ channel opening. The activity of $InsP_3R1$ is under feedback control by cytosolic Ca^{2+}; at low Ca^{2+} concentrations, Ca^{2+} acts as co-activator of the $InsP_3R1$, and at higher Ca^{2+} concentrations the $InsP_3R1$ is inhibited by Ca^{2+} (Bezprozvanny et al., 1991; Finch et al., 1991; Iino, 1990; Kaznacheyeva et al., 1998). This property of $InsP_3R1$, called *bell-shaped* Ca^{2+} dependence, is essential for generation of Ca^{2+} waves and Ca^{2+} oscillations (Berridge, 1993; De Young and Keizer, 1992; Lechleiter and Clapham, 1992; Parker et al., 1996). Despite crucial importance for the $InsP_3R1$ signaling function, very little is known about structural determinants and mechanisms responsible for the $InsP_3R1$ regulation by cytosolic Ca^{2+}.

The ryanodine receptor (RyanR) is another Ca^{2+}-gated intracellular Ca^{2+} release channel with distant sequence homology to the $InsP_3R$ (Furuichi et al., 1994). All three mammalian isoforms of the RyanR share a conserved glutamate residue in the putative Ca^{2+}-sensor region—E3885 in RyanR3, E4032 in RyanR1, and E3987 in RyanR2. This critical glutamate is conserved in the RyanR family from *Caenorhabditis elegans* to mammalian isoforms (Fig. 1). Point mutations of the conserved glutamate to alanine induced 1000- to 3000-fold reduction in the RyanR2 sensitivity to Ca^{2+} activation (Li and Chen, 2001), and >10,000-fold reduction in the RyanR3 sensitivity to Ca^{2+} activation (Chen et al., 1998). Analogous mutation of RyanR1 abolished channel activity (Du and MacLennan, 1998). The $InsP_3R$ gene family is homologous to the RyanR family in the putative Ca^{2+}-sensor region and also contains a conserved glutamate residue (Miyakawa et al., 2001; see also Fig. 1, this article). In the rat $InsP_3R1$ the conserved glutamate is located at position 2100 (E2100) (Fig. 1). Using DT40 cell expression system and Ca^{2+} imaging assay, in the previous work we demonstrated that E2100D mutation resulted in ~10-fold decrease in the $InsP_3R1$ sensitivity to Ca^{2+} activation (Miyakawa et al., 2001).

In the present study we performed further biochemical and functional characterization of the putative $InsP_3R1$ Ca^{2+} sensor. Using intrinsic tryptophan fluorescence spectroscopy we determined Ca^{2+}-binding affinity of the wild-type and E2100 mutant putative $InsP_3R1$ Ca^{2+}-sensor region. Obtained biochemical results were correlated with the functional analysis of the wild-type $InsP_3R1$ and E2100 mutants in planar lipid bilayers. The results obtained in our study support the hypothesis that E2100 residue forms a part of the $InsP_3R1$ Ca^{2+} sensor.

Submitted January 28, 2003, and accepted for publication March 20, 2003.

Address reprint requests to Dr. Ilya Bezprozvanny, Dept. of Physiology, K4.112, UT Southwestern Medical Ctr. at Dallas, 5323 Harry Hines Blvd., Dallas, TX 75390-9040. Tel.: 214-648-6737; Fax: 214-648-2974; E-mail: Ilya.Bezprozvanny@UTSouthwestern.edu.

0006-3495/03/07/290/10 $2.00

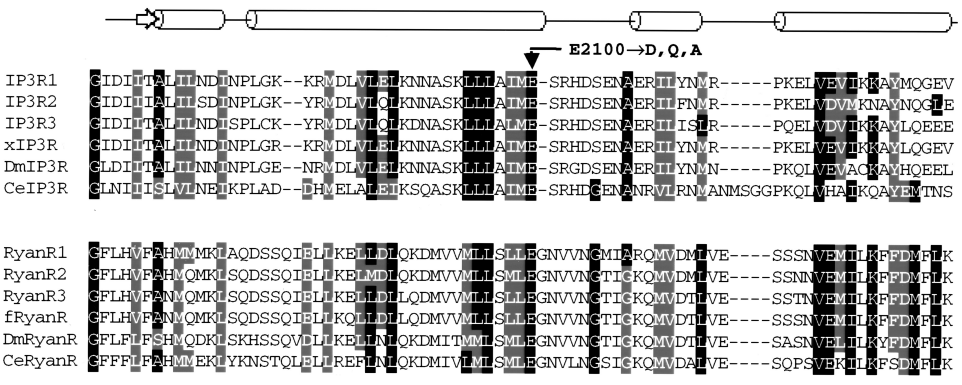

FIGURE 1 Alignment of the putative cytosolic Ca^{2+} sensor for the InsP$_3$R and RyanR gene families. The sequence of rat InsP$_3$R1 (P29994, amino acids 2061–2133) is aligned with the corresponding region of rat InsP$_3$R2 (P29995), rat InsP$_3$R3 (Q63269), *Xenopus* InsP$_3$R (Q91908), *Drosophila* InsP$_3$R (P29993), and *C. elegans* InsP$_3$R (Q9Y0A1). The sequence of rabbit RyanR1 (P11716, amino acids 3991–4067) is aligned with the corresponding region of rabbit RyanR2 (P30957), rabbit RyanR3 (Q9TS33), bullfrog RyanR (Q91319), *Drosophila* RyanR (Q24498), and *C. elegans* RyanR (P91905). The sequence alignment was performed by ClustalW and the residues conserved between InsP$_3$R and RyanR gene families were shaded by BOXSHADE. The secondary structure prediction for the InsP$_3$R Ca^{2+}-sensor region performed by PSIPRED is shown above the alignment. PSIPRED predicts nearly identical secondary structure for the RyanR Ca^{2+}-sensor region (not shown). The conserved glutamate residue (E2100 in InsP$_3$R1) mutated in the previous (Miyakawa et al., 2001) and in the present work is indicated.

MATERIALS AND METHODS

Expression and purification of the putative InsP$_3$R1 Ca^{2+}-sensor region

The putative Ca^{2+}-sensor region (E1932–R2270) of rat InsP$_3$R1 (Mignery et al., 1990) was amplified by PCR and cloned into XbaI/XhoI sites of pGEX-KG (Amersham-Pharmacia Biotech, Piscataway, NJ) bacterial expression vector to generate GST-RT1-Cas (Calcium-sensor) construct. The GST-E2100D-Cas and GST-E2100Q-Cas constructs were generated using the same procedure on the basis of InsP$_3$R1-E2100D and InsP$_3$R1-E2100Q mutants (Miyakawa et al., 2001). Generated constructs were verified by sequencing and transformed into protease-deficient BL21 bacterial expression host strain. Recombinant GST-RT1-Cas, GST-E2100D-Cas, and GST-E2100Q-Cas fusion proteins were expressed in 2 liters of BL21 cells by 0.8 mM isopropyl β-*d*-thiogalactoside induction at 15°C. The cells were harvested 20 h postinduction and resuspended in 50 ml of the lysis buffer (50 mM Imidasole pH 7.0, 100 mM NaCl, 10 mM EDTA, 1 mM DTT, 0.5 mg/ml lysozyme, 1% Triton X-100) with addition of the protease inhibitors. The cells were disrupted by sonication (Branson Sonifier 450, VWR USA, West Chester, PA), clarified by centrifugation at 15,000 rpm (Beckman JA-10) and incubated with 2 ml of glutathione-sepharose 4B beads (Amersham-Pharmacia Biotech). The glutathione-sepharose 4B beads were pelleted at 2000 rpm, washed with 5 volumes of the low salt buffer (20 mM Imidasole pH 7.0, 100 mM NaCl, 1 mM EDTA, 1 mM DTT) and the high salt buffer (20 mM Imidasole pH 7.0, 1M NaCl, 1mM EDTA, 1 mM DTT, 0.1% sodium azide). The GST-RT1-Cas, GST-E2100D-Cas, and GST-E2100Q-Cas fusion proteins attached to glutathione-sepharose 4B beads were resuspended in 2 ml of PBS (pH 7.35), mixed with 100 μL of thrombin solution (100 Thrombin cleavage units), incubated at room temperature for 4 h with constant mixing and centrifuged at 2000 rpm. Obtained supernatants were collected, transferred to fresh tubes, and diluted by PBS to the total volume of 6 ml. Resulting samples of RT1-Cas, E2100D-Cas, and E2100Q-Cas recombinant proteins were analyzed by SDS-PAGE electrophoresis and Coomassie staining.

Intrinsic tryptophan fluorescence spectroscopy

Intrinsic tryptophan fluorescence spectroscopy of RT1-Cas, E2100D-Cas, and E2100Q-Cas recombinant proteins was performed immediately after thrombin cleavage using a DeltaRAM Illuminator (Photon Technology International, Lawrenceville, NJ). During these measurements, a quartz cuvette containing 2 ml of recombinant proteins at 80 μg/ml in PBS was supplemented with 1 mM EGTA and 1 mM HEDTA (pH 7.35). The free Ca^{2+} concentration in the cuvette was adjusted in the range of pCa 9.4–2 by consecutive additions of calibrated $CaCl_2$ stock solutions with constant stirring. The free Ca^{2+} concentration in the cuvette was calculated using MaxChelator (http://www.stanford.edu/~cpatton/maxc.html). Intrinsic tryptophan fluorescence was excited by 280-nm (2-nm slit width) light, and emission spectra were collected at room temperature in the 290- to 500-nm range with 2-nm step size. The experiments were controlled and analyzed by the Felix software package (Photon Technology International).

The absolute peak tryptophan fluorescence values at each Ca^{2+} concentration were determined from the generated emission spectra ($F(Ca^{2+})$). The measured fluorescence values were corrected for dilution F_{cor} $(Ca^{2+}) = F_0/(1 + v/V)$, where F_{cor} (Ca^{2+}) is dilution-corrected fluorescence value, F_0 is a peak fluorescence value with no $CaCl_2$ added (pCa 9.4), v is a total volume of $CaCl_2$ added, and V is a starting solution volume in the cuvette (2 ml). The difference between measured and dilution-corrected peak tryptophan fluorescence values $\Delta F(Ca^{2+}) = F(Ca^{2+}) - F_{cor}(Ca^{2+})$ was taken as a measure of Ca^{2+}-induced conformational changes in RT1-Cas, E2100D-Cas, and E2100Q-Cas recombinant proteins (Ward, 1985). The ΔF values at each Ca^{2+} concentration were normalized to the maximal ΔF value (ΔF_{max}) measured at pCa 2.0 in the same experiment. The normalized ΔF values from three independent experiments for each recombinant protein were averaged together. The Ca^{2+} dependence of the normalized and averaged ΔF values were fit by the least-squares method (Microcal Origin 4.1) using the Hill equation $\Delta F/\Delta F_{max}$ $(Ca^{2+}) = [Ca^{2+}]^n/([Ca^{2+}]^n + k_{Ca}{}^n)$, where $[Ca^{2+}]$ is a Ca^{2+} concentration in the cuvette, n is a Hill coefficient, and k_{Ca} is an apparent affinity for Ca^{2+}. Resulting k_{Ca} and n-values for RT1-Cas, E2100D-Cas, and E2100Q-Cas recombinant proteins are presented in the text. The confidence range of k_{Ca} and n-values was determined from the quality of the fit.

Generation of recombinant baculoviruses

Generation of recombinant baculovirus expressing wild-type rat InsP$_3$R1 (RT1) was previously described (Nosyreva et al., 2002; Tu et al., 2002). The E2100D and E2100Q mutations of InsP$_3$R1 in pIRES2-EGFP vector were previously described (Miyakawa et al., 2001). The 2.5 kb BamH1/BamH1 fragment (3797, 6329) of InsP$_3$R1 sequence containing E2100D and E2100Q mutations was isolated and subcloned into BamH1 digested and CIAP-dephosphorylated pFastBac1-InsP$_3$R1 plasmid with EcoR1, BamH1, Xho1, Kpn1, and Sph1 sites removed from the polylinker sequence. The orientation of BamH1/BamH1 fragment was verified by PCR and the presence of E2100D and E2100Q mutations in resulting pFastBac1-E2100D and pFastBac1-E2100Q plasmids was verified by sequencing. The recombinant E2100D and E2100Q baculoviruses encoding InsP$_3$R1-

E2100D and $InsP_3R1$-E2100Q mutants were generated and amplified using Bac-to-Bac system (Invitrogen, Carlsbad, CA) as described previously for the RT1 virus (Nosyreva et al., 2002; Tu et al., 2002) to yield baculoviral stock of 10^8–10^9 pfu/ml titer.

Expression of $InsP_3R1$ mutants in Sf9 cells

The $InsP_3R1$ mutants were expressed in *Spodoptera frugiperda* (Sf9) cells as previously described (Nosyreva et al., 2002; Tu et al., 2002). Briefly, Sf9 cells were obtained from ATCC and cultured in suspension culture in supplemented Grace's Insect Media with 10% FBS at 27°C. For the $InsP_3R1$ expression, 150 ml of Sf9 cell cultures were infected by RT1, E2100D, and E2100Q baculovirus at MOI of 5–10. 66 h postinfection, Sf9 cells were collected by centrifugation at 4°C for 5 min at 800 rpm (GH 3.8 rotor, Beckman Instruments, Fullerton, CA). The cellular pellet was resuspended in 25 ml of homogenization buffer (Sucrose 0.25 M, HEPES 5 mM, pH 7.4) supplemented with protease inhibitors cocktail (1mM EDTA, aprotinin 2 μg/ml, leupeptin 10 μg/ml, benzamidine 1 mM, AEBSF 2.2 mM, pepstatin 10 μg/ml, and PMSF 0.1 mg/ml). Cells were disrupted by sonication (Branson Ultrasonics, Danbury, CT) and manually homogenized on ice with glass-Teflon homogenizer. The microsomes were isolated from Sf9 cell homogenate by gradient centrifugation as previously described for HEK293 cells (Kaznacheyeva et al., 1998). The final microsomal preparation was resuspended in 0.5 ml of the storage buffer (10% sucrose, 10 mM MOPS pH 7.0) to yield typically 6 mg/ml of protein (Bradford assay, Bio-Rad, Hercules, CA), aliquoted, quickly frozen in liquid nitrogen and stored at −80°C. Expression of $InsP_3R1$ wild-type E2100D and E2100Q mutants was confirmed by Western blotting. The anti-$InsP_3R1$ rabbit polyclonal antibody (T_{443}) was previously described (Kaznacheyeva et al., 1998).

Single channel recordings and analysis of the mutant $InsP_3R1$ activity

Recombinant RT1, E2100D, and E2100Q channels expressed in Sf9 cells were incorporated into the bilayer by microsomal vesicle fusion as previously described (Nosyreva et al., 2002; Tu et al., 2002). Single channel currents were recorded at 0 mV transmembrane potential using 50 mM Ba^{2+} dissolved in HEPES (pH 7.35) in the *trans* (intraluminal) side as a charge carrier (Bezprozvanny and Ehrlich, 1994). The *cis* (cytosolic) chamber contained 110 mM Tris dissolved in HEPES (pH 7.35). To obtain Ca^{2+} dependence of the $InsP_3R$ we follow the protocol from Bezprozvanny et al. (1991). Free Ca^{2+} concentration in the *cis* chamber was controlled in the range 10 nM (pCa 8) to 10 μM (pCa 5) by mixture of 1 mM EGTA, 1 mM HEDTA, and variable concentrations of $CaCl_2$. The resulting free Ca^{2+} concentration was calculated by using a program described in Fabiato (1988). All recordings of $InsP_3R1$ activity were performed in the presence of 0.5 mM Na_2ATP (Bezprozvanny and Ehrlich, 1993) and 2 μM $InsP_3$. All additions ($InsP_3$, ATP, and $CaCl_2$) were to the *cis* chamber from the concentrated stocks with at least 30-s stirring of solutions in both chambers. The $InsP_3R1$ single-channel currents were amplified (Warner Instruments OC-725, Hamden, CT), filtered at 1 kHz by low pass 8-pole Bessel filter, digitized at 5 kHz (Digidata 1200, Axon Instruments) and stored on computer hard drive and recordable optical discs.

For off-line computer analysis (pClamp 7, Axon Instruments, Foster City, CA), single-channel data were filtered digitally at 500 Hz; for presentation of the current traces, data were filtered at 200 Hz. Evidence for the presence of two to three functional channels in the bilayer was obtained in the majority of experiments. The number of active channels in the bilayer was estimated as a maximal number of simultaneously open channels during the course of an experiment (Horn, 1991). The open probability of closed level, and first and second open levels, was determined by using half-threshold crossing criteria ($t \geq 2$ ms) from the records lasting at least 2.5 min. The single-channel open probability (P_o) for one channel was calculated using the binomial distribution for the levels 0, 1, and 2, and assuming that the channels were identical and independent (Colquhoun and Hawkes, 1983).

To generate complete Ca^{2+}-dependence curves, the experiments with persistent $InsP_3R1$ activity for duration of the experiment (>30 min) were chosen for analysis to prevent artifacts related to irreversible channel inactivation occasionally observed in the bilayers. To construct Ca^{2+}-dependence curves for the wild-type and mutant $InsP_3R1$, the determined values of P_o were averaged across several independent experiments at each Ca^{2+} concentration. The averaged values of P_o are presented as mean ± SE (n = number of independent experiments) and fit by the least-squares methods (Sigma Plot 5, Jandel Scientific, San Rafael, CA) using the bell-shaped equation $P_o([Ca^{2+}]) = 4P_m k^n[Ca^{2+}]^n/((k^n + [Ca^{2+}]^n)(K^n + [Ca^{2+}]^n)$, modified from Bezprozvanny et al. (1991), where P_m is a parameter proportional to the maximal P_o value, n is a Hill coefficient, k is the apparent affinity of the Ca^{2+} activating site, and K is the apparent affinity of the Ca^{2+} inhibitory site. The parameters of the optimal fit (P_m, n, k, and K) for each $InsP_3R1$ form are presented in the text. The confidence range of k- and K-values was determined from the quality of the fit. The fitting procedure used in this article differs from the procedure used in our previous articles (Bezprozvanny et al., 1991; Kaznacheyeva et al., 1998; Nosyreva et al., 2002; Tu et al., 2002), in that P_o values in the present article were not normalized to the maximal P_o before averaging and fitting. Because P_o values were not normalized, P_m is equal to maximal P_o only in the case when $k = K$. If $k \neq K$, parameter P_m is proportional (and higher) than maximal P_o.

RESULTS

Ca^{2+} binding to the putative $InsP_3R1$ Ca^{2+}-sensor region

Our previous Ca^{2+} imaging experiments suggested an importance of E2100 residue in $InsP_3R1$ modulation by Ca^{2+} (Miyakawa et al., 2001). Based on these results we reasoned that the part of the $InsP_3R1$ sequence surrounding E2100 residue forms the $InsP_3R1$ Ca^{2+} sensor. To test this hypothesis, we expressed and purified the putative $InsP_3R1$ Ca^{2+}-sensor region RT1-Cas (E1932–R2270, Fig. 2 *A*) as described in Methods. The amino-terminal boundary of RT1-Cas construct (E1932) was chosen based on the limited trypsin digest pattern of the $InsP_3R1$ (Yoshikawa et al., 1999). The carboxyl-terminal boundary (R2270) was chosen by the proximity of the first $InsP_3R1$ transmembrane domain M1 (S2276–Y2294, Fig. 2 *A*). To investigate the effects of E2100 mutations, we also expressed and purified E2100D-Cas and E2100Q-Cas proteins (see Methods). Similar yield of RT1-Cas, E2100D-Cas, and E2100Q-Cas proteins was achieved in our experiments (Fig. 2 *B*, *gel*). The mobility of these proteins on SDS-gel was consistent with the predicted molecular weight of 39 kDa (Fig. 2 *B*, *gel*), indicating that the full-length RT1-Cas, E2100D-Cas, and E2100Q-Cas proteins were obtained in our expression/purification scheme.

The putative $InsP_3R1$ Ca^{2+}-sensor region contains two tryptophan residues (W2255 and W2267) and 11 tyrosine residues. The fluorescence emission spectra (excitation at 280 nm) of RT1-Cas protein displayed a well-defined peak at 332 nm (Fig. 3 *A*), consistent with a partially buried position of W2255 and W2267 residues in the hydrophobic core of RT1-Cas protein. We reasoned that binding of Ca^{2+} may

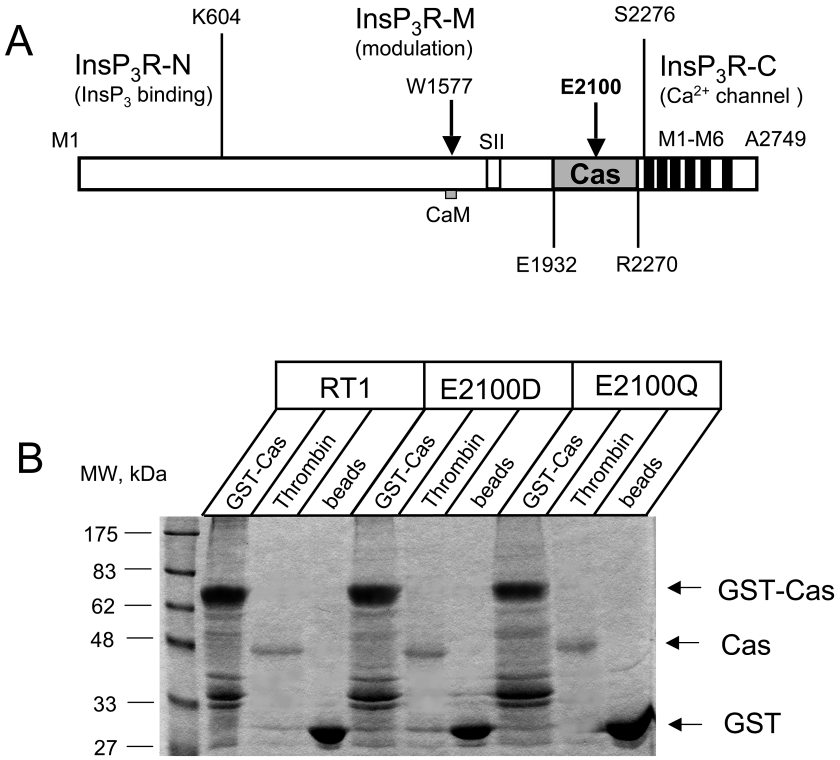

FIGURE 2 Expression and purification of the putative $InsP_3R1$ Ca^{2+}-sensor region. (*A*) Domain structure of the $InsP_3R1$ (adapted from Mignery and Sudhof, 1990). The boundaries of the amino-terminal $InsP_3$-binding domain $InsP_3R$-N (1–604), the carboxyl-terminal channel-forming domain $InsP_3R$-C (2276-2749) with transmembrane domains M1–M6, the middle coupling domain $InsP_3R$-M (605–2275) are indicated. The putative $InsP_3R1$ Ca^{2+}-sensor region Cas (1932–2270) is shaded. The mutations of E2100 residue (Miyakawa et al., 2001), W1577 residue (CaM-binding site; see Nosyreva et al., 2002), and the alternative splicing in SII site (Tu et al., 2002) were previously analyzed. (*B*) Expression and purification of the putative $InsP_3R1$ Ca^{2+}-sensor region. Samples of GST-Cas attached to glutathione beads (*GST-Cas*), Cas proteins released by thrombin cleavage (*Thrombin*), and glutathione beads after thrombin cleavage (*beads*) were analyzed by SDS-PAGE gel electrophoresis (10% polyacrylamide gel stained with Coomassie Blue). The predicted molecular weight of GST-Cas (68 kDa), Cas (39 kDa), and GST (29 kDa) are indicated by the arrows. 1/60 (*GST-Cas* and *beads lanes*) or 1/200 (*thrombin lanes*) of total protein was loaded on the gel for RT1, E2100D, and E2100Q.

induce a conformation change of RT1-Cas fragment which may affect intrinsic tryptophan fluorescence signal (Ward, 1985). A similar approach has been taken recently in studies of NEFA Ca^{2+} binding (Kroll et al., 1999) and apolipophorin III proton binding (Weers et al., 2001). To test this hypothesis, we collected emission spectra (excitation at 280 nm) of RT1-Cas protein at different Ca^{2+} concentrations (pCa 9.4–pCa 2.0, buffered by 1 mM EGTA and 1 mM HEDTA). We found that the position of the emission peak (λ_{max}) remained constant at 332 nm (Fig. 3 *A*). However, a systematic and saturable change in the intensity of RT1-Cas fluorescent signal as a function of Ca^{2+} was observed (Fig. 3 *A*). To compare the data from different experiments, the observed changes in RT1-Cas peak fluorescence intensity (ΔF) were corrected for dilution, normalized to the maximal change in the peak fluorescence intensity (ΔF_{max}), averaged, and plotted against Ca^{2+} concentration (Fig. 4, *open circles*). Best fit to the average RT1-Cas data (Fig. 4, *curve*) yielded an apparent Ca^{2+}-binding affinity k_{Ca} of 0.16 $\pm$ 0.02 μM Ca^{2+} and Hill coefficient n of 0.54 $\pm$ 0.02 (Table 1).

What are the effects of E2100 mutations on affinity of putative $InsP_3R1$ Ca^{2+} sensor for Ca^{2+}? To answer this question, we collected tryptophan fluorescence emission spectra of E2100D-Cas and E2100Q-Cas recombinant proteins at different Ca^{2+} concentrations. Similar to the experiments with RT1-Cas (Fig. 3 *A*), we observed a systematic and saturable Ca^{2+}-dependent change in the intensity of E2100D-Cas and E2100Q-Cas intrinsic fluorescent signals (Fig. 3, *B* and *C*). Just as with RT1-Cas, the λ_{max} of E2100D-Cas and E2100Q-Cas emission spectra remained constant at 332 nm (Fig. 3, *B* and *C*). The observed changes in E2100D-Cas and E2100Q-Cas peak fluorescence intensity (ΔF) were corrected for dilution, normalized, and averaged as described for RT1-Cas. Best fit to the average E2100D-Cas and E2100Q-Cas data (Fig. 4, *filled circles* and *open triangles*) yielded $k_{Ca} = 1.0 \pm 0.3$ μM Ca^{2+}, $n = 0.49 \pm 0.04$ for E2100D-Cas; and $k_{Ca} = 1.1 \pm 0.3$ μM Ca^{2+}, $n = 0.45 \pm 0.05$ for E2100Q-Cas (Table 1).

Functional expression of $InsP_3R1$ E2100 mutants in Sf9 cells

Mutations of E2100 residue resulted in five- to sixfold reduction in the affinity of $InsP_3R1$ putative Ca^{2+} sensor for Ca^{2+} (Figs. 3 and 4, Table 1). What are the effects of E2100 mutations on $InsP_3R1$ modulation by Ca^{2+}? Previously we addressed this question in Ca^{2+} imaging studies with the DT40 cell expression system (Miyakawa et al., 2001). To gain an additional insight into the significance of E2100 residue for the $InsP_3R1$ function, we took an advantage of our ability to measure single-channel activity of recombinant $InsP_3R1$ expressed in Sf9 cells (Nosyreva et al., 2002; Tu et al., 2002). To analyze the functional effect of E2100 mutations on $InsP_3R1$ activity at the single-channel level, we generated RT1, E2100D, and E2100Q baculoviruses as described in Methods. Microsomes isolated from Sf9 cells infected with RT1, E2100D, and E2100Q baculoviruses, but

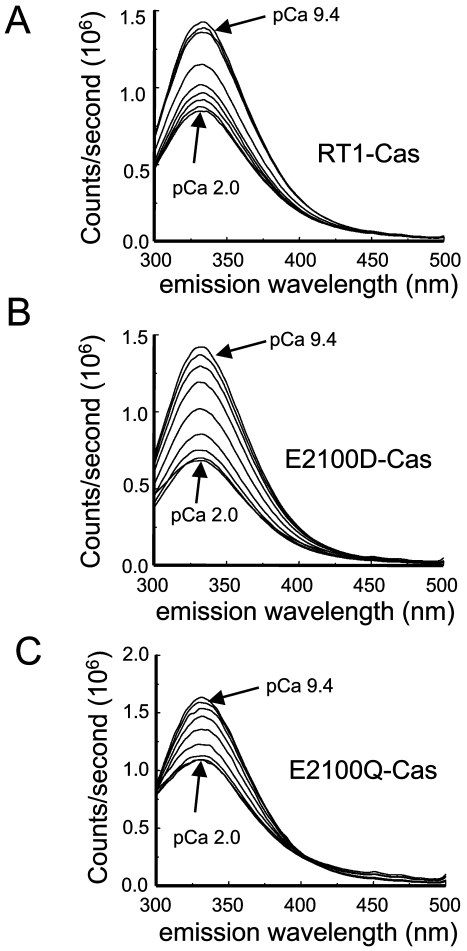

FIGURE 3 Intrinsic tryptophan fluorescence emission spectra of the putative $InsP_3R1$ Ca^{2+}-sensor region. Representative intrinsic tryptophan fluorescence emission spectra of RT1-Cas (*A*), E2100D-Cas (*B*), and E2100Q-Cas (*C*) proteins at variable Ca^{2+} concentrations (pCa 9.4–pCa 2.0, as indicated). Similar results were obtained in at least three independent experiments with RT1-Cas, E2100D-Cas, and E2100Q-Cas proteins.

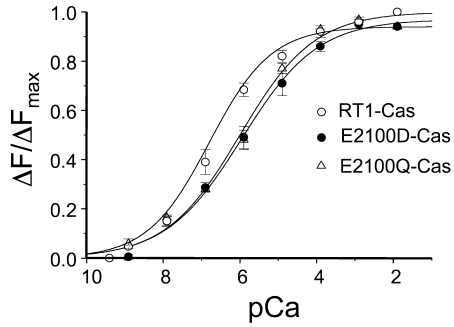

FIGURE 4 Ca^{2+} binding to the putative $InsP_3R1$ Ca^{2+}-sensor region. Dilution-corrected and normalized changes in the peak fluorescence intensity ($\Delta F/\Delta F_{max}$) were averaged together at each Ca^{2+} concentration and shown as mean ± SE ($n = 3$) for RT1-Cas (*open circles*), E2100D-Cas (*filled circles*), and E2100Q-Cas (*open triangles*). The data were fit by the Hill equation (see Methods). The parameters of the optimal fits (*smooth curves*) are presented in Table 1.

not from noninfected cells, contained large quantities of $InsP_3R1$ detectable by Western blotting (Fig. 5). Small amounts of endogenous $InsP_3R1$ were detected in microsomes from noninfected Sf9 cells when the blots were overexposed (data not shown). The apparent molecular size of recombinant RT1 and E2100 mutants was identical to the $InsP_3R1$ present in rat cerebellar microsomes (Fig. 4 *A*). The immunopositive bands of smaller molecular weight detected in samples of rat cerebellar microsomes and microsomes from RT1-infected Sf9 cells correspond to products of partial $InsP_3R1$ proteolysis. When expressed in Sf9 cells, E2100Q appears to be somewhat more sensitive to proteolysis than RT1 and E2100D (Fig. 5).

When microsomes isolated from Sf9 cells infected with RT1, E2100D, and E2100Q baculoviruses were fused to planar lipid bilayers, functional $InsP_3$-gated channels were recorded (Fig. 6). The $InsP_3$-gated channels were observed in 15 out of 20 experiments with RT1, in 16 out of 20 experiments with E2100D, and in 15 out of 22 experiments with E2100Q. The $InsP_3$-gated channels were never ($n = 5$) observed in experiments with the microsomes from noninfected Sf9 cells, and we concluded that endogenous $InsP_3R$ background in Sf9 cells does not interfere with recordings of recombinant $InsP_3R1$ activity. At pCa 6.7 and in the presence of 0.5 mM ATP and 2 μM $InsP_3$ (standard recording conditions), the mean open time was 5.8 ± 0.4 ms ($n = 4$) for RT1 (Fig. 6 *A*), 6.8 ± 0.1 ms ($n = 4$) for E2100D (Fig. 6 *B*), and 7.8 ± 0.4 ms ($n = 3$) for E2100Q (Fig. 6 *C*). In the same conditions the unitary current amplitude at 0 mV transmembrane potential was 2.0 ± 0.1 pA ($n = 4$) for RT1 (Fig. 6 *A*), 1.8 ± 0.1 pA ($n = 4$) for E2100D (Fig. 6 *B*), and 1.8 ± 0.1 pA ($n = 3$) for E2100Q (Fig. 6 *C*). Thus, in standard recording conditions the E2100D and E2100Q

TABLE 1 Parameters of the biochemical and functional analysis of the $InsP_3R1$ Ca^{2+} sensor

	Ca^{2+} Binding		Bell-shaped Ca^{2+} Dependence				
$InsP_3R1$ isoform	Affinity for Ca^{2+} K_{Ca} (μM)	Hill coefficient n	P_m	Hill coefficient n	Affinity of the activating site k (μM)	Affinity of the inhibitory site K (μM)	Peak of Ca^{2+} dependence (pCa)
RT1	0.16 ± 0.02	0.54 ± 0.02	0.30	1.3	0.22 ± 0.01	0.20 ± 0.01	6.71
E2100D	1.0 ± 0.3	0.49 ± 0.04	0.27	1.2	1.11 ± 0.07	1.85 ± 0.10	5.81
E2100Q	1.1 ± 0.3	0.45 ± 0.05	0.27	0.9	1.44 ± 0.14	0.94 ± 0.09	5.94

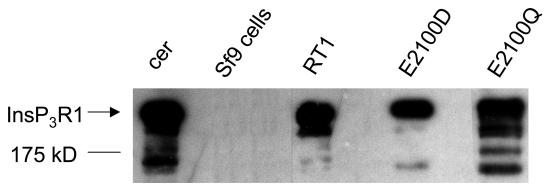

FIGURE 5 Expression of RT1 and E2100 mutants in Sf9 cells. Rat cerebellum microsomes (*cer*) and microsomes isolated from noninfected SF9 cells (*Sf9 cells*), and Sf9 cells infected with RT1, E2100D, and E2100Q baculoviruses, were analyzed by Western blotting with the anti-InsP$_3$R1 polyclonal antibody. For each microsomal preparation, 20 μg of total protein was loaded on the gel.

mutations resulted in 10% reduction in the unitary current size and 20–30% increase in the open dwell time when compared to RT1. In our previous study we discovered that an alternative splicing of SII region and *opt* mutation in the InsP$_3$R1-coupling domain affect InsP$_3$R1 single-channel conductance (Tu et al., 2002). Thus, in contrast to the generally accepted domain structure of InsP$_3$R1 (Mignery and Sudhof, 1990), the InsP$_3$R1 unitary current size appears to be sensitive to changes in the primary sequence of the InsP$_3$R1 modulatory region.

Modulation of InsP$_3$R1 and E2100 mutants by cytosolic Ca^{2+}

Bell-shaped Ca^{2+} dependence of InsP$_3$R1 activity on cytosolic Ca^{2+} (Bezprozvanny et al., 1991; Finch et al., 1991; Iino, 1990) is one of the most fundamental InsP$_3$R1 properties responsible for complex spatiotemporal aspects of Ca^{2+} signaling (Berridge, 1993). In the next series of experiments we evaluated modulation of recombinant rat InsP$_3$R1 by cytosolic Ca^{2+}. We found that RT1 channels display bell-shaped Ca^{2+} dependence with the maximal open probability at 200 nM Ca^{2+}, half-maximal activation at 100 nM Ca^{2+}, and half-inhibition at 1 μM Ca^{2+} (Fig. 7). These results are in agreement with the behavior of native cerebellar InsP$_3$R (Bezprozvanny et al., 1991), recombinant rat InsP$_3$R1 expressed in HEK-293 and COS cells (Kaznacheyeva et al., 1998; Ramos-Franco et al., 1998), and with our previous findings with the InsP$_3$R1 expressed in Sf9 cells (Nosyreva et al., 2002; Tu et al., 2002). To obtain quantitative description of RT1 Ca^{2+} dependence, the data from four independent experiments were averaged together and fit by the bell-shaped equation modified from Bezprozvanny et al. (1991) as described in Methods. The parameters of the optimal Ca^{2+}-dependence fit (Fig. 7 *B*, *smooth curve*) are presented in Table 1. From the fit we estimated that for RT1 channels, the apparent affinities of Ca^{2+}-activating and Ca^{2+}-inhibitory sites are 0.22 $\pm$ 0.01 μM and 0.20 $\pm$ 0.01 μM Ca^{2+}, respectively (Table 1).

Using DT40 cell expression system and Ca^{2+} imaging assay, in the previous article we demonstrated that E2100D mutation resulted in ~10-fold decrease in the InsP$_3$R1 sensitivity to Ca^{2+} activation, but could not analyze inhibitory portion of E2100D Ca^{2+} dependence (Miyakawa et al., 2001). In the same study we also established that E2100Q forms a functional InsP$_3$-sensitive channel, but could not determine E2100Q Ca^{2+} dependence (Miyakawa et al., 2001). Here, we took advantage of our ability to perform single-channel recordings of E2100D and E2100Q channels (Fig. 6, *B* and *C*), and determined complete Ca^{2+} dependence of E2100 mutants in planar lipid bilayers. We found that both E2100D (Fig. 8) and E2100Q (Fig. 9) displayed bell-shaped Ca^{2+} dependence. When compared to RT1, the bell-shaped Ca^{2+} dependence of both E2100D and E2100Q was shifted

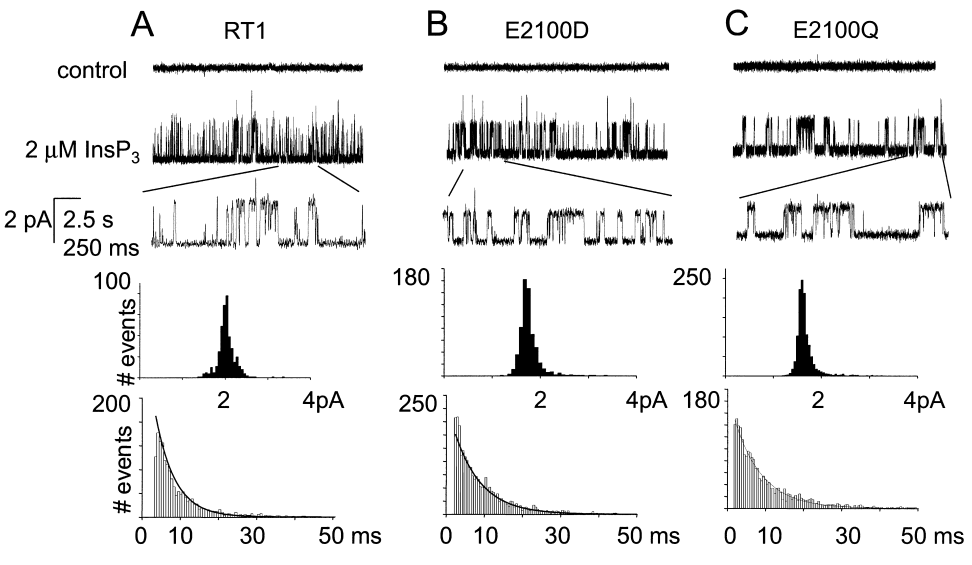

FIGURE 6 Single-channel properties of RT1 and E2100 mutants. Representative channel activity of RT1 (*A*), E2100D (*B*), and E2100Q (*C*) recorded in the presence of 0.2 μM Ca^{2+}, 0.5 mM Na$_2$ATP, and 2 μM InsP$_3$ (standard recording conditions). Current records are shown at compressed and expanded timescales as indicated. Unitary current amplitude histograms and open dwell time distributions from the same experiment are shown below the current records. Unitary currents were fitted with a Gaussian function that was centered at 2.0 pA for RT1, 1.7 pA for E2100D, and 1.6 pA for E2100Q. Open time distributions were fit with a single exponential function (*curve*) that yielded a τ_0 of 5.3 ms for RT1, 6.9 ms for E2100D, and 7.3 ms for E2100Q. Similar analysis was performed for at least three independent experiments with RT1, E2100D, and E2100Q.

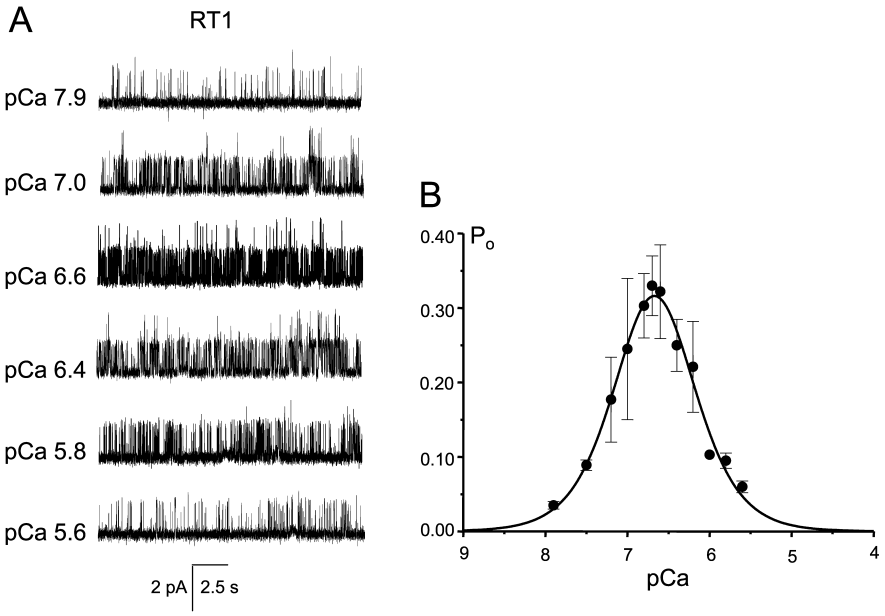

FIGURE 7 RT1 Ca^{2+} dependence. (*A*) The current recordings of RT1 from the same experiment at different Ca^{2+} concentrations as indicated. (*B*) Bell-shaped Ca^{2+} dependence of the RT1 channels. The data from independent experiments were averaged together at each Ca^{2+} concentration as described in Methods, and shown as mean ± SE ($n = 4$; *filled circles*). The averaged data were fitted by the bell-shaped equation modified from Bezprozvanny et al. (1991) as explained in Methods. The parameters of optimal fit (*smooth curve*) are in Table 1.

to ~sevenfold higher Ca^{2+} concentrations, with the peak at 1.5 μM Ca^{2+} (Figs. 8 *B* and 9 *B*). To obtain a quantitative description of E2100D and E2100Q Ca^{2+} dependence, the data from several experiments ($n = 4$ for E2100D and $n = 3$ for E2100Q) were averaged together and fit by the modified bell-shaped equation as described in Methods. The parameters of the optimal Ca^{2+} dependence fits (Figs. 8 *B* and 9 *B*, *thick smooth curves*) are presented in Table 1. From the fit we determined that in E2100D and E2100Q mutants the apparent affinity of both Ca^{2+}-activating and Ca^{2+} inhibitory sites was decreased from 0.2 μM Ca^{2+} to 1–2 μM Ca^{2+} (Table 1).

DISCUSSION

An importance of E2100 residue for $InsP_3R1$ modulation by Ca^{2+} was demonstrated in Ca^{2+} imaging experiments described in our previous article (Miyakawa et al., 2001). From these results we proposed that the region surrounding E2100 residue serves as a putative Ca^{2+} sensor of the $InsP_3R1$. In the present article we tested this hypothesis by a combination of biochemical and functional methods. Using $^{45}Ca^{2+}$ overlay assay, a Ca^{2+}-binding site has been previously detected in a heterologously expressed 1961–2220 region of rat $InsP_3R1$ (Mignery et al., 1992). A number of additional Ca^{2+}-binding sites in the $InsP_3R1$ sequence

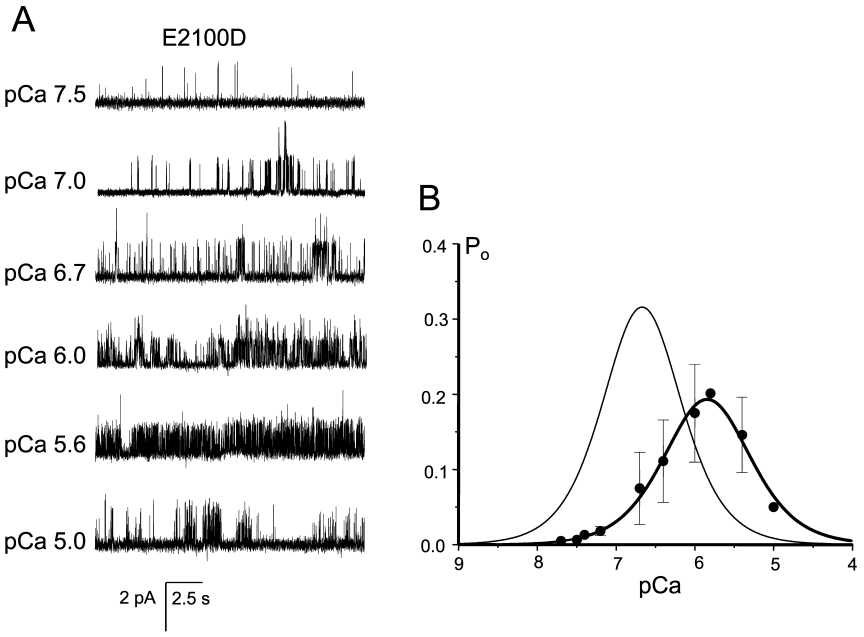

FIGURE 8 E2100D Ca^{2+} dependence. (*A*) The current recordings of E2100D mutant from the same experiment at different Ca^{2+} concentrations as indicated. (*B*) Bell-shaped Ca^{2+} dependence of E2100D mutant. The data from independent experiments were averaged together at each Ca^{2+} concentration as described in Methods and shown as mean ± SE ($n = 4$) (*filled circles*). The averaged data were fitted by the bell-shaped equation modified from Bezprozvanny et al. (1991) as explained in Methods. The parameters of optimal fit (*smooth thick curve*) are in Table 1. The thin smooth line represents RT1 Ca^{2+} dependence from Fig. 7 *B*.

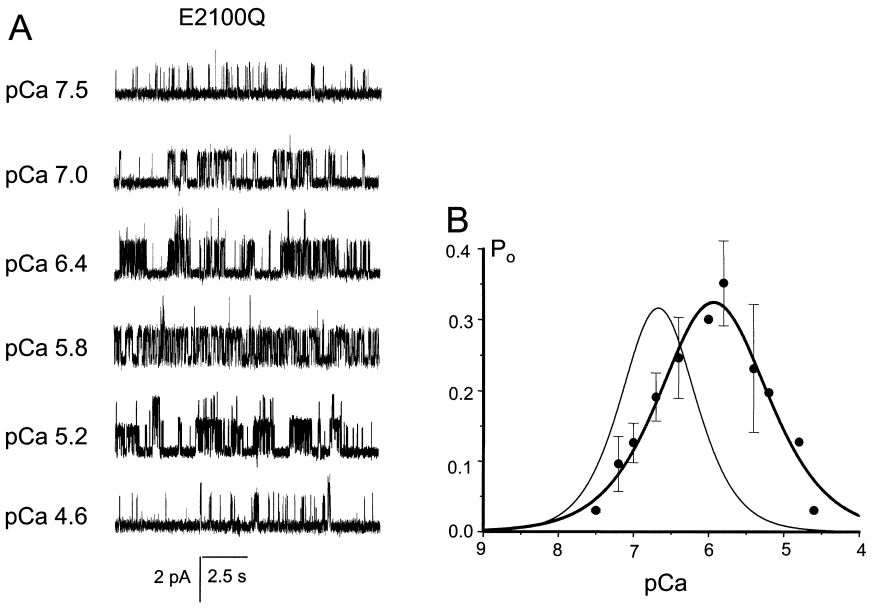

FIGURE 9 E2100Q Ca^{2+} dependence. (*A*) The current recordings of E2100Q mutant from the same experiment at different Ca^{2+} concentrations as indicated. (*B*) Bell-shaped Ca^{2+} dependence of E2100Q mutant. The data from independent experiments were averaged together at each Ca^{2+} concentration as described in Methods, and shown as mean ± SE ($n = 3$; *filled circles*). The averaged data were fitted by the bell-shaped equation modified from Bezprozvanny et al. (1991) as explained in Methods. The parameters of optimal fit (*smooth thick curve*) are in Table 1. The thin smooth line represents RT1 Ca^{2+} dependence from Fig. 7 *B*.

were discovered using a similar approach (Sienaert et al., 1996, 1997), including a site in the region between 2124–2146 amino acids with 0.8 μM affinity for Ca^{2+}. Mutation of E2139 residue located within this region had no effect on Ca^{2+} sensitivity of the InsP$_3$R1 expressed in DT-40 cells (Miyakawa et al., 2001), but it is possible that this or other motifs may also contribute to Ca^{2+} binding in the regulatory site of the InsP$_3$R1. Using intrinsic tryptophan fluorescence assay, here we demonstrated that the putative InsP$_3$R1 Ca^{2+}-sensor region (E1932–R2270, Fig. 2 *A*) forms Ca^{2+}-binding site with the affinity of 0.16 μM Ca^{2+} (Figs. 3 and 4, Table 1). The Hill coefficient of 0.5 measured in our experiments (Fig. 4, Table 1) indicates a negative cooperativity in association of InsP$_3$R1 putative Ca^{2+}-sensor region with Ca^{2+}, which may be due to multimerization of recombinant proteins during our measurements or due to the presence of multiple Ca^{2+}-binding sites within the InsP$_3$R1 putative Ca^{2+}-sensor region. Further experiments will be needed to discriminate between these possibilities.

The E2100 residue is highly conserved in the InsP$_3$R gene family from *C. elegans* to mammalian isoforms (Fig. 1). The homologous glutamate residue in the RyanR gene family is also highly conserved (Fig. 1) and has been shown to play a critical role in RyanR activation by Ca^{2+} for RyanR2 (Li and Chen, 2001) and RyanR3 (Chen et al., 1998). Thus, both families of Ca^{2+} release channels appear to employ similar molecular mechanism for Ca^{2+}-dependent gating. Secondary structure prediction for the InsP$_3$R Ca^{2+}-sensor region (Fig. 1) and for the corresponding region of RyanR (data not shown) suggests that the conserved glutamate residue (E2100 in InsP$_3$R1) is located at the tip of a long α-helix followed by a loop-helix-loop-helix motif. Interestingly, the part of the long α-helix immediately preceding the conserved glutamate residue is very hydrophobic and highly conserved between InsP$_3$R and RyanR gene families (Fig. 1). Similar helix-loop-helix unit often forms a part of Ca^{2+}-binding site in proteins (Kawasaki and Kretsinger, 1995) and it is likely that the Ca^{2+}-sensor region of InsP$_3$R and RyanR contains a similar fold. Three-dimensional structure determination of the corresponding InsP$_3$R/RyanR region will help to test the latter hypothesis.

Our fluorescence measurements indicate that the association with Ca^{2+} induces a conformational change of the putative InsP$_3$R1 Ca^{2+}-sensor region that quenches intrinsic tryptophan fluorescence signal (Figs. 3 and 4). It is likely that in the context of the full-length InsP$_3$R1 the observed conformational changes are linked to the InsP$_3$R1 gating mechanism. We also concluded that both E2100D and E2100Q mutations reduced the affinity of the putative InsP$_3$R1 Ca^{2+}-sensor region for Ca^{2+} ~five- to sixfold, to 1 μM Ca^{2+} (Figs. 3 and 4, Table 1). Thus, in agreement with our hypothesis (Miyakawa et al., 2001), the E2100 residue indeed plays a critical role in function of InsP$_3$R1 Ca^{2+} sensor. One explanation of these results is that E2100 residue plays a direct role in coordinating a Ca^{2+} ion. In this case we have to assume that the role of E2100 residue in Ca^{2+} coordination is lost to an equal degree in both E2100D and E2100Q mutants, presumably due to compensation by other residues. An alternative explanation is that E2100 residue plays an important role in maintaining an overall structure of InsP$_3$R1 Ca^{2+}-binding site, and that both E2100D and E2100Q mutations disrupt this structure to a similar degree. Importantly, the peak of intrinsic tryptophan emission spectra for RT1, E2100D, and E2100Q fragments was positioned at the same $\lambda_{max} = 332$ nm, indicating that the overall secondary and tertiary structure of the InsP$_3$R1 putative Ca^{2+}-sensor region is maintained in E2100 mutants. The intrinsic tryptophan fluorescence measurements described here can

be used to search for other residues important for Ca^{2+} binding to $InsP_3R1$ Ca^{2+} sensor. Ultimately, a solution of three-dimensional structure of $InsP_3R1$ Ca^{2+}-sensor region will be required to determine the exact role played by E2100 residue and to identify the residues involved in coordinating a Ca^{2+} ion.

The importance of E2100 residue for $InsP_3R1$ modulation by Ca^{2+} was further supported in functional experiments performed with recombinant $InsP_3R1$ channels reconstituted into planar lipid bilayers. We discovered that E2100D and E2100Q mutations shifted the sensitivity of $InsP_3R1$ to activation by Ca^{2+} ~sevenfold when compared to RT1 channels (Figs. 7–9). From these experiments we estimated that the apparent affinity of Ca^{2+} activating site was equal to 0.22 μM Ca^{2+} for RT1 (Fig. 7, Table 1), and 1.1–1.5 μM Ca^{2+} for E2100D and E2100Q (Figs. 8 and 9, and Table 1). Thus, the apparent affinities of $InsP_3R1$ activating Ca^{2+}-binding site estimated for RT1, E2100D, and E2100Q channels from current recordings are in good agreement with the $InsP_3R1$ putative Ca^{2+}-sensor-binding affinities determined in intrinsic tryptophan fluorescence measurements (Table 1). Our data with E2100D mutant are in agreement with the previous functional analysis in DT40 cells (Miyakawa et al., 2001). In the previous article we found that sensitivity of $InsP_3R1$ to activation by Ca^{2+} is shifted by a factor of ~10 with the peak at ~3 μM Ca^{2+} (Miyakawa et al., 2001). We also found that BCR activation in DT40 cells expressing E2100D mutant leads to a single Ca^{2+} spike, in contrast to Ca^{2+} oscillations observed in wild-type $InsP_3R1$-expressing cells (Miyakawa et al., 2001). These results suggest that sensitivity of $InsP_3R1$ to Ca^{2+} is important for Ca^{2+} dynamics in living cells. The data obtained with E2100 mutants in the present study (Fig. 8) are in quantitative agreement with results from DT40 cells (Miyakawa et al., 2001). Only a small fraction of E2100Q expression DT40 cells responded to BCR stimulation, and responses were low in amplitude (Miyakawa et al., 2001). Thus the Ca^{2+} dependence of E2100Q mutant could not be analyzed in the study with DT40 cells (Miyakawa et al., 2001). Here we were able to obtain functional recordings of E2100Q channels in bilayers and discovered that Ca^{2+} sensitivity of E2100Q channels is similar to Ca^{2+} sensitivity of E2100D channels (Fig. 9). Thus, weak response in E2100Q-transfected DT40 cells are not likely to be due to an additional shift in Ca^{2+}-sensitivity and most likely results from insufficient expression or misassembly of E2100Q mutants in DT40 cells. In agreement with this hypothesis, the E2100Q channels were recorded in bilayers less frequently than the wild-type or E2100D channels, indicating that many E2100Q proteins do not form functional channels when expressed in Sf9 cells.

Interestingly, mutations of E2100 residue affected not only the Ca^{2+}-activating site, but also the Ca^{2+}-inhibitory site of the $InsP_3R1$ (Figs. 7–9, and Table 1). The inhibitory portion of E2100D Ca^{2+} dependence has not been previously analyzed due to limitations of the Ca^{2+} imaging method (Miyakawa et al., 2001). An original formal mathematical description of cerebellar $InsP_3R$ bell-shaped Ca^{2+} dependence assumed independent binding of Ca^{2+} to activating and inhibitory sites present on each $InsP_3R1$ subunit (Bezprozvanny et al., 1991). The physical basis for this model is that a number of Ca^{2+} ions bound to the activating and inhibitory binding sites on each $InsP_3R1$ subunit has a combined effect on $InsP_3R1$ open probability. Similar assumption was made in the more recent mathematical analysis of *Xenopus* $InsP_3R$ biphasic Ca^{2+} dependence (Mak et al., 1998). Thus, the effect of E2100 mutations on the apparent affinity of $InsP_3R1$ Ca^{2+} inhibitory site was unexpected. One potential explanation to this finding is offered by a sequential Ca^{2+}-binding model (Bezprozvanny, 1994; Finch et al., 1991; Othmer and Tang, 1993; Taylor, 1998), according to which Ca^{2+} inhibitory site is exposed only after Ca^{2+} is bound in the activating site. Another possible explanation of our results is that E2100 forms a part of both activating and inhibitory Ca^{2+}-binding sites. The molecular identity of $InsP_3R1$ inhibitory Ca^{2+}-binding site is controversial. Calmodulin has been strongly implicated in Ca^{2+}-dependent inhibition of cerebellar $InsP_3R1$ (Michikawa et al., 1999). However, recent data suggested that the high affinity Ca^{2+}-calmodulin-binding site in the coupling region of $InsP_3R1$ (Yamada et al., 1995) does not play a direct role in the biphasic modulation of $InsP_3R1$ by Ca^{2+} (Nosyreva et al., 2002; Zhang and Joseph, 2001). Thus, the Ca^{2+} inhibitory site can be a part of $InsP_3R1$ sequence, which may include E2100. Future experiments with additional $InsP_3R1$ Ca^{2+}-sensor mutants will be required to test these and other potential hypotheses.

We are grateful to Gregory Mignery and Thomas C. Südhof for the kind gift of the rat $InsP_3R1$ clone, and to Phil Thomas for advice and encouragement with tryptophan fluorescence measurements. We are thankful to Phyllis Foley for the administrative assistance and to Anton Maximov and Humbert De Smedt for comments on the manuscript.

Supported by the Welch Foundation, the National Institutes of Health grant R01 NS38082 (to I.B.), and by a grant from the Ministry of Education, Culture, Sports, Science and Technology of Japan (to M.I.).

REFERENCES

Berridge, M. J. 1993. Inositol trisphosphate and calcium signalling. *Nature*. 361:315–325.

Bezprozvanny, I. 1994. Theoretical analysis of calcium wave propagation based on inositol (1,4,5)-trisphosphate ($InsP_3$) receptor functional properties. *Cell Calcium*. 16:151–166.

Bezprozvanny, I., and B. E. Ehrlich. 1993. ATP modulates the function of inositol 1,4,5-trisphosphate-gated channels at two sites. *Neuron*. 10: 1175–1184.

Bezprozvanny, I., and B. E. Ehrlich. 1994. Inositol (1,4,5)-trisphosphate ($InsP_3$)-gated Ca channels from cerebellum: conduction properties for divalent cations and regulation by intraluminal calcium. *J. Gen. Physiol.* 104:821–856.

Bezprozvanny, I., and B. E. Ehrlich. 1995. The inositol 1,4,5-trisphosphate ($InsP_3$) receptor. *J. Membr. Biol.* 145:205–216.

Bezprozvanny, I., J. Watras, and B. E. Ehrlich. 1991. Bell-shaped calcium-response curves of $Ins^{1,4,5}P_3$- and calcium-gated channels from endoplasmic reticulum of cerebellum. *Nature.* 351:751–754.

Chen, S. R., K. Ebisawa, X. Li, and L. Zhang. 1998. Molecular identification of the ryanodine receptor Ca^{2+} sensor. *J. Biol. Chem.* 273:14675–14678.

Colquhoun, D., and A. G. Hawkes. 1983. The principles of stochastic interpretation of ion-channel mechanisms. *In* Single-Channel Recording. B. Sakmann and E. Neher, editors. Plenum Press, New York. 135–174.

De Young, G. W., and J. Keizer. 1992. A single pool IP_3-receptor-based model for agonist stimulated Ca2+ oscillations. *Proc. Natl. Acad. Sci. USA.* 89:9895–9899.

Du, G. G., and D. H. MacLennan. 1998. Functional consequences of mutations of conserved, polar amino acids in transmembrane sequences of the Ca^{2+} release channel (ryanodine receptor) of rabbit skeletal muscle sarcoplasmic reticulum. *J. Biol. Chem.* 273:31867–31872.

Fabiato, A. 1988. Computer programs for calculating total from specified free or free from specified total ionic concentrations in aqueous solutions containing multiple metals and ligands. *Methods Enzymol.* 157: 378–417.

Finch, E. A., T. J. Turner, and S. M. Goldin. 1991. Calcium as a coagonist of inositol 1,4,5-trisphosphate-induced calcium release. *Science.* 252:443–446.

Furuichi, T., K. Kohda, A. Miyawaki, and K. Mikoshiba. 1994. Intracellular channels. *Curr. Opin. Neurobiol.* 4:294–303.

Horn, R. 1991. Estimating the number of channels in patch recordings. *Biophys. J.* 60:433–439.

Iino, M. 1990. Biphasic Ca^{2+} dependence of inositol 1,4,5-trisphosphate-induced Ca release in smooth muscle cells of the guinea pig *taenia caeci*. *J. Gen. Physiol.* 95:1103–1122.

Kawasaki, H., and R. H. Kretsinger. 1995. Calcium-binding proteins 1: EF-hands. *Prot. Prof.* 2:297–490.

Kaznacheyeva, E., V. D. Lupu, and I. Bezprozvanny. 1998. Single-channel properties of inositol (1,4,5)-trisphosphate receptor heterologously expressed in HEK-293 cells. *J. Gen. Physiol.* 111:847–856.

Kroll, K. A., S. Otte, G. Hirschfeld, S. Barnikol-Watanabe, H. Gotz, H. Sternbach, H. D. Kratzin, H. U. Barnikol, and N. Hilschmann. 1999. Heterologous overexpression of human NEFA and studies on the two EF- hand calcium-binding sites. *Biochem. Biophys. Res. Commun.* 260:1–8.

Lechleiter, J. D., and D. E. Clapham. 1992. Molecular mechanisms of intracellular calcium excitability in *Xenopus laevis* oocytes. *Cell.* 69:283–294.

Li, P., and S. R. Chen. 2001. Molecular basis of Ca^{2+} activation of the mouse cardiac Ca^{2+} release channel (ryanodine receptor). *J. Gen. Physiol.* 118:33–44.

Mak, D. O., S. McBride, and J. K. Foskett. 1998. Inositol 1,4,5-trisphosphate activation of inositol trisphosphate receptor Ca^{2+} channel by ligand tuning of Ca^{2+} inhibition. *Proc. Natl. Acad. Sci. USA.* 95:15821–15825.

Michikawa, T., J. Hirota, S. Kawano, M. Hiraoka, M. Yamada, T. Furuichi, and K. Mikoshiba. 1999. Calmodulin mediates calcium-dependent inactivation of the cerebellar type 1 inositol 1,4,5-trisphosphate receptor. *Neuron.* 23:799–808.

Mignery, G. A., P. A. Johnston, and T. C. Sudhof. 1992. Mechanism of Ca^{2+}-inhibition of $InsP_3$ binding to the cerebellar $InsP_3$ receptor. *J. Biol. Chem.* 267:7450–7455.

Mignery, G. A., C. L. Newton, B. T. Archer, and T. C. Sudhof. 1990. Structure and expression of the rat inositol 1,4,5-trisphosphate receptor. *J. Biol. Chem.* 265:12679–12685.

Mignery, G. A., and T. C. Sudhof. 1990. The ligand binding site and transduction mechanism in the inositol-1,4,5-triphosphate receptor. *EMBO J.* 9:3893–3898.

Miyakawa, T., A. Maeda, T. Yamazawa, K. Hirose, T. Kurosaki, and M. Iino. 1999. Encoding of Ca^{2+} signals by differential expression of IP_3 receptor subtypes. *EMBO J.* 18:1303–1308.

Miyakawa, T., A. Mizushima, K. Hirose, T. Yamazawa, I. Bezprozvanny, T. Kurosaki, and M. Iino. 2001. Ca^{2+}-sensor region of IP_3 receptor controls intracellular Ca^{2+} signaling. *EMBO J.* 20:1674–1680.

Nosyreva, E., T. Miyakawa, Z. Wang, L. Glouchankova, A. Mizushima, M. Iino, and I. Bezprozvanny. 2002. The high affinity calcium-calmodulin-binding site does not play a role in modulation of type 1 inositol (1,4,5)-trisphosphate receptor function by calcium and calmodulin. *Biochem. J.* 365:659–667.

Othmer, H. G., and Y. Tang. 1993. Oscillations and waves in a model of $InsP_3$-controlled calcium dynamics. *In* Experimental and Theoretical Advances in Biological Pattern Formation. H. G. Othmer, editor. Plenum Press, New York. 277–299.

Parker, I., J. Choi, and Y. Yao. 1996. Elementary events of $InsP_3$-induced Ca^{2+} liberation in *Xenopus* oocytes: hot spots, puffs and blips. *Cell Calcium.* 20:105–121.

Ramos-Franco, J., S. Caenepeel, M. Fill, and G. Mignery. 1998. Single channel function of recombinant type-1 inositol 1,4,5-trisphosphate receptor ligand binding domain splice variants. *Biophys. J.* 75:2783–2793.

Sienaert, I., H. De Smedt, J. B. Parys, L. Missiaen, S. Vanlingen, H. Sipma, and R. Casteels. 1996. Characterization of a cytosolic and a luminal Ca^{2+} binding site in the type I inositol 1,4,5-trisphosphate receptor. *J. Biol. Chem.* 271:27005–27012.

Sienaert, I., L. Missiaen, H. De Smedt, J. B. Parys, H. Sipma, and R. Casteels. 1997. Molecular and functional evidence for multiple Ca^{2+}-binding domains in the type 1 inositol 1,4,5-trisphosphate receptor. *J. Biol. Chem.* 272:25899–25906.

Taylor, C. W. 1998. Inositol trisphosphate receptors: Ca^{2+}-modulated intracellular Ca^{2+} channels. *Biochim. Biophys. Acta.* 1436:19–33.

Thrower, E. C., R. E. Hagar, and B. E. Ehrlich. 2001. Regulation of $Ins_{1,4,5}P_3$ receptor isoforms by endogenous modulators. *Trends Pharmacol. Sci.* 22:580–586.

Tu, H., T. Miyakawa, Z. Wang, L. Glouchankova, M. Iino, and I. Bezprozvanny. 2002. Functional characterization of the type 1 inositol 1,4,5-trisphosphate receptor coupling domain SII(+/−) splice variants and the *opisthotonos* mutant form. *Biophys. J.* 82:1995–2004.

Ward, L. D. 1985. Measurement of ligand binding to proteins by fluorescence spectroscopy. *Methods Enzymol.* 117:400–414.

Weers, P. M., C. M. Kay, and R. O. Ryan. 2001. Conformational changes of an exchangeable apolipoprotein, apolipophorin III from *Locusta migratoria*, at low pH: correlation with lipid binding. *Biochemistry.* 40:7754–7760.

Yamada, M., A. Miyawaki, K. Saito, T. Nakajima, M. Yamamoto-Hino, Y. Ryo, T. Furuichi, and K. Mikoshiba. 1995. The calmodulin-binding domain in the mouse type 1 inositol 1,4,5-trisphosphate receptor. *Biochem. J.* 308:83–88.

Yoshikawa, F., H. Iwasaki, T. Michikawa, T. Furuichi, and K. Mikoshiba. 1999. Trypsinized cerebellar inositol 1,4,5-trisphosphate receptor. Structural and functional coupling of cleaved ligand binding and channel domains. *J. Biol. Chem.* 274:316–327.

Zhang, X., and S. K. Joseph. 2001. Effect of mutation of a calmodulin binding site on Ca^{2+} regulation of inositol trisphosphate receptors. *Biochem. J.* 360:395–400.